

Journal of Materials Chemistry A

Accepted Manuscript



This is an *Accepted Manuscript*, which has been through the Royal Society of Chemistry peer review process and has been accepted for publication.

Accepted Manuscripts are published online shortly after acceptance, before technical editing, formatting and proof reading. Using this free service, authors can make their results available to the community, in citable form, before we publish the edited article. We will replace this *Accepted Manuscript* with the edited and formatted *Advance Article* as soon as it is available.

You can find more information about *Accepted Manuscripts* in the [Information for Authors](#).

Please note that technical editing may introduce minor changes to the text and/or graphics, which may alter content. The journal's standard [Terms & Conditions](#) and the [Ethical guidelines](#) still apply. In no event shall the Royal Society of Chemistry be held responsible for any errors or omissions in this *Accepted Manuscript* or any consequences arising from the use of any information it contains.



Journal Name

ARTICLE

Low-energy formate production from CO₂ electroreduction using electrodeposited tin on GDE

Received 00th January 20xx,
Accepted 00th January 20xx

DOI: 10.1039/x0xx00000x

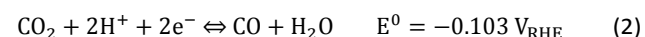
www.rsc.org/

E. Irtem^a, T. Andreu^{a,b,*}, A. Parra^a, M.D. Hernandez-Alonso^c, S. García-Rodríguez^c, J.M. Riesco-García^c, G. Penelas-Pérez^c, J.R. Morante^{a,b}

Tin electrodeposition on carbon fibers have been implemented as gas diffusion electrode for electroreduction of CO₂ to formate in a flow electrochemical cell design. Unlike other approaches, this method does not incorporate any additive or binder in the electrode improving their catalytic performances. Once optimized, the system shows an improved dependence of the effective production formate yield by surface and time units, mol m⁻² s⁻¹, on the consumed energy by mol, W h mol⁻¹. It reduces the formic acid production energy cost requiring less than 250 W h mol⁻¹, with formate faradaic efficiency as high as 71% being fully stable at least for 6 hours.

1. Introduction

In order to move towards a circular economy which implies to reduce waste to a minimum, overturning the concept of CO₂ as a pollutant, instead exploring its value as a feedstock through CO₂ reduction techniques, emerge as an interesting opportunity. In this context, the electroreduction of CO₂ (CO₂R) in aqueous media is particularly interesting and feasible as water based electrolytes can be used as proton source, and the reaction is conducted at room temperature.¹ For that, on one hand, it is important to promote CO₂R over competing hydrogen evolution reaction (HER) to guarantee the efficient production of reduced CO₂ products. Furthermore, at least CO and HCOOH can compete as reduction compounds among CO₂R:²



In order to favor the formic acid production the difference among energy barriers needs to be compensated using a catalyst that favors the formation of formic acid over the other products. Many researchers have reported results of CO₂R into formate (HCOO⁻) on different metal catalysts such as Sn, Pb, Bi and In.³⁻⁸ The cause of their selectivity to formate were related

to their large overpotential for hydrogen evolution giving enough room for stabilization of intermediate steps for formate production, i.e. (i) by formation of free or weakly adsorbed CO₂^{•-} followed (ii) by proton attack to the carbon atom.⁹ Among these catalyst candidates Sn appears to be the most abundant and environment friendly.

Furthermore, the low CO₂ solubility (0.034 M) in aqueous solution is also an important issue. Therefore, a gas diffusion electrode (GDE) with disperse catalyst material is desirable in order to minimize the mass transport limitations and improve the availability of the three phase interfaces (TPI) which is the meeting point of CO₂ gas – liquid electrolyte – electrode where the catalyst reaction will take place.

Among the different potential CO₂ reduced subproducts, formate or formic acid has been receiving great industrial attention because of their versatility in various applications (e.g., direct formic acid fuel cells,¹⁰ leather, textile, chemical and food industries). Likewise, its production from CO₂ electrochemical reduction appears as a powerful alternative as long as the energy consumption is kept low enough during the electrosynthesis as well as in the posterior concentration procedure to reach the background purity of commercial formic, typically 85% in weight.¹¹ This parameter is especially relevant for ensuring the economic viability of the process. Moreover, in order to decrease investment costs the use of inexpensive electrodes materials with high degradation endurance is basic too. The price of the formic acid metric ton is currently around 1000€ with an estimated annual increase of about 2%. In this scenario, according to the existing literature¹²⁻¹⁵ nowadays, the high faradaic efficiency values are obtained with energy consumptions per mol higher than 300 W h whereas the combustion energy under standard conditions associated to formic acid is -254.6 kJ mol⁻¹ (70.7 W h mol⁻¹).

^a Department of Advanced Materials for Energy, Catalonia Institute for Energy Research (IREC), Jardins de les Dones de Negre, 1, 08930 Sant Adrià de Besòs, Catalonia, Spain.

^b Universitat de Barcelona (UB), Martí i Franquès, 1, 08028 Barcelona, Catalonia, Spain.

^c Repsol Technology Center, C/ Agustín de Betancourt s/n, 28935 Móstoles, Madrid, Spain.

* Corresponding author. E-mail: tandreu@irec.cat

Electronic Supplementary Information (ESI) available: See

DOI: 10.1039/x0xx00000x

Recent efforts have been paid on the implementation of GDE for CO₂R. In this way, high density of active sites should be available in a three-dimensional network of conductive supporting material allowing simultaneously CO₂ gas diffusion and charge transfer. Typically, a catalyst layer consisted of Sn nanopowders and/or SnO₂ film with Nafion® solution and propanol to disperse the components (with carbon black, carbon nanotubes or graphene) drop cast on a glassy carbon (GC) electrode or sprayed on a gas diffusion layer has received attention due to an enhanced efficiency caused by the use of the nanosized electrocatalyst, obtaining results of faradaic efficiency for formate are ranging between 65 to 73 %, although consumed energy by mol is not yet enough improved.^{4, 14-24} (a summary is given in Table S1). Consequently, important efforts are still needed for simultaneously improve degradation endurance, maintain high faradaic efficiencies for formate concentration and decrease the required energy consumption for formic acid synthesis. All these conditions must be fulfilled to satisfy the minimum requirements for its industrial applicability foresight. Beyond these aspects, only few studies in the literature have been addressed toward the influence of the gas and electrolyte flow rates on the production yield in an up-scalable and continuous flow cell using GDE^{25, 26} considering the final concentration of the product in the catholyte.

In this work, a CO₂ gas diffusion electrode based on submicron Sn catalyst particles obtained by electrodeposition onto the carbon fibers of the GDE was used as cathode to convert CO₂ into formate (HCOO⁻) with a high CO₂R faradaic efficiency that achieves around 85%, of which 71% corresponds to sodium formate. In contrast to previous studies, there is not an additive used such as a conductive powder or additional binder in the gas diffusion electrode that extend the foreseen life time increasing degradation endurance. This electrode has been used as improved cathode in a stacked flow cell system that combines a well-defined electrode – electrolyte (membrane) – electrode interface working close to each other to increase the diffusion of ions and decrease the cell resistance. At the same time, based on the continuous system, gas/liquid flow ratio can be adequately modified to optimize formate production. Unlike previous proposed approaches^{4, 13-16, 26-28}, this developed system and procedure is shown to have lower energy consumption by mol, (<250 W h mol⁻¹), for competitive formate effective production yields, in the range 2-4 10⁻⁴ mol m⁻² s⁻¹.

2. Experimental

2.1. Catalyst preparation and characterization

Tin catalysts (Sn-GDE) were obtained by electrodeposition on carbon fibers using conventional three electrode cell configuration. A sheet of carbon paper (Toray® carbon paper, TGP-H-60) with a size of 30 x 34 mm was used as catalyst support (working electrode), the counter electrode was 40 x 40 mm graphite foil (0.5mm thick, 99.8%, Alfa Aesar) and Ag/AgCl/KCl(3M) ($E^0 = 0.203 \text{ V}_{\text{NHE}}$) was used as a reference

electrode. A pyrophosphate bath containing 0.40 M K₄P₂O₇, 0.09 M Sn₂P₂O₇ and 0.05 M C₄H₆O₆ was used as electrolyte for tin electrodeposition.²⁹ To enhance mass transport and prevent side reactions such as oxygen reduction reaction, argon gas was continuously bubbled during the plating process. The electrodeposition was carried out using a Biologic SP-150 potentiostat working under galvanostatic mode, applying a current density of 15 mA cm⁻² during 5 min at room temperature. After electrodeposition, each electrode was thoroughly rinsed with deionized water and dried in vacuum oven (25 Torr, Ar atmosphere) at 70°C for 2 h.

Structural characterization was carried out by X-ray diffraction (XRD) in a D8 Advance Bruker equipment with a Cu K_{α1} radiation source working at 40 kV and 40 mA with the samples being scanned from $2\theta = 10^\circ$ to 80° at a rate of 0.02 s⁻¹ in Bragg–Brentano geometry. Morphology of the as deposited Sn-GDE was observed using a Zeiss (Auriga) scanning electron microscope (SEM) and elemental analysis was performed by the same microscope equipped with an Oxford X-ray energy dispersive spectrometer (EDS).

2.2. Electrolysis cell and experimental set-up

Carbon dioxide electroreduction experiments were carried out in a filter-press type electrochemical cell (Micro Flow Cell, Electrocell A/S), where a Dimensionally Stable Anode plate (DSA/O₂, Electrocell S/A) was used as anode and Sn-GDE was used as a cathode. An ionic transport membrane (Nafion® 117) divided the cell in two separated anodic and cathodic compartments. A leak-free Ag/AgCl 3.4 M KCl reference electrode (Warner Instruments) was assembled in a polytetrafluoroethylene (PTFE) frame of the cell, placed very close to the cathode surface. As seen in Figure 1, the cell had three inputs (catholyte, anolyte and CO₂) and two outputs (catholyte+CO₂ and anolyte). Anolyte (0.5M NaOH, Panreac, >98%) and catholyte (0.5M NaHCO₃, Merck >99.9%, pre-electrolysed at -2V under nitrogen bubbling to remove metal impurities) were kept in two separated tanks and recirculated continuously to the cell by a dual peristaltic pump (Major Science, MU-D02) to accumulate liquid products. A mass flow controller (Bronkhorst F-201CV) was used to control CO₂ flow rate entering the system, measured downstream by a volumetric digital flowmeter Agilent ADM 2000. The flow of CO₂ gas and electrolytes were kept at 10 mL min⁻¹ unless otherwise specified (gas-to-liquid ratio of 1). The experiments were carried out under potentiostatic conditions in two-

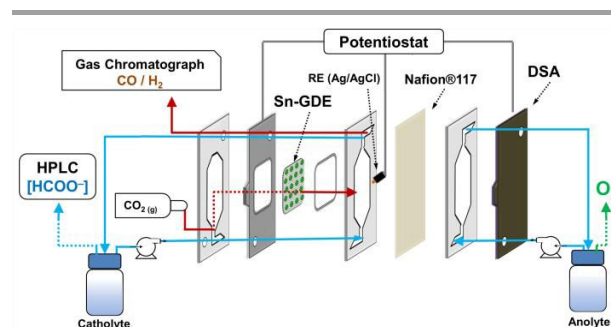


Figure 1. Scheme of the electrochemical flow cell

electrode configuration, applying a voltage between anode and cathode, using a potentiostat/galvanostat Biologic VMP3. A second potentiostat/galvanostat Biologic VMP3 was used to monitor in three-electrode configuration the voltage of each electrode versus the Ag/AgCl reference electrode. For the sake of clarity, potential was transformed to the reversible hydrogen electrode (RHE) scale: $E(V_{\text{RHE}}) = E(V_{\text{Ag/AgCl}}) + 0.0592\text{pH} + 0.203$.

The faradaic efficiency to formate is the percentage of the total charge supplied that is used to produce formate. For its quantification, a total charge of 4 C mL^{-1} of catholyte (typical 50 mL) was employed for the electrolysis to assure a measurable quantity of formate at every potential. The product in the liquid phase was analyzed, after acidification, by High Performance Liquid Chromatography system (HPLC, Perkin Elmer Flexar SQ300MS) equipped with a Rezex ROA-Organic Acid H+ (8%) column ($300 \times 7.8\text{ mm}$, Phenomenex), with an isocratic pump ($2.5\text{ mM H}_2\text{SO}_4$, 6 mL min^{-1}) and a UV Detector set at 210 nm. Analogously, carbon monoxide and hydrogen faradaic efficiencies were calculated using the analysis of the outlet gas by gas chromatography (GC) using a multichannel Agilent 490 microGC equipped with two Molsieve columns with argon carrier for hydrogen analysis and with helium carrier for carbon monoxide analysis.

3. Results and discussion

3.1. Tin catalyst immobilized by electrodeposition

Tin catalysts (Sn-GDE) were obtained by electrodeposition on carbon fibers using a pyrophosphate bath. One of the advantage of the pyrophosphate solution is its pH close to neutrality ($\text{pH} = 8$) and then tartaric acid additive as complexing agent allows deposits to be obtained with a uniform morphology by favoring Sn metal reduction over hydrogen evolution (HER). As seen in the cyclic voltammetry (Figure 2), the reduction of Sn^{2+} to Sn on carbon fiber electrode starts at $-0.13\text{ V}_{\text{RHE}}$ close to its standard redox potential,² while HER is significantly retarded. Cathodic scan of the cyclic voltammogram shows a plateau near 20 mA cm^{-2} because of tin reduction reaches a limiting current density. Later, a significant hydrogen formation was detected from $-1.32\text{ V}_{\text{RHE}}$.

In order to understand the deposition mechanism, we have applied five current values ranging from 1 to 30 mA cm^{-2} . For all deposited samples the charge density was kept constant (4.5 C cm^{-2}) which gives rise to coverage of the carbon fibers located in the front part of the gas diffusion electrode. Depending on the used current density, the nucleation and distribution of the layer deposited onto the carbon fibers changes as well as the depth of the achieved coverage. Due to the nucleation, growth and deposition rates, the procedure from 1 to 6 mA cm^{-2} did not uniformly cover the fibers, (Figure S1), while, a current density that exceeds the limiting current density like 30 mA cm^{-2} give rise to Sn particles forming needle-like deposits with poor mechanical adherence due to concomitant hydrogen evolution. These deposits peel off

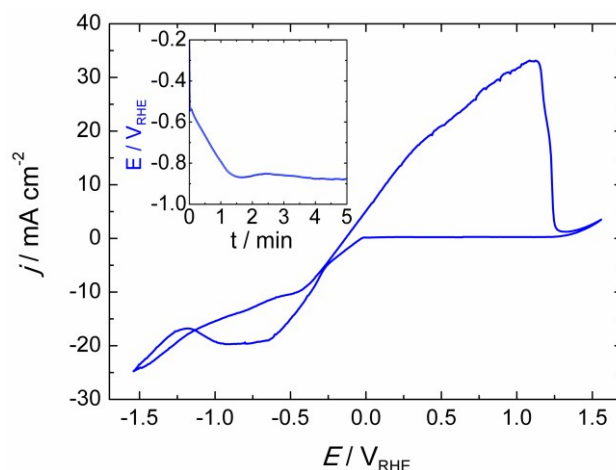


Figure 2. Cyclic voltammogram for tin deposition and stripping on gas diffusion electrode (C-Toray TGP-H-60) in pyrophosphate bath ($\text{pH } 8.3$) at a scan rate of 20 mV s^{-1} . Insert, chronopotentiometry at 15 mA cm^{-2} during Sn catalyst deposition.

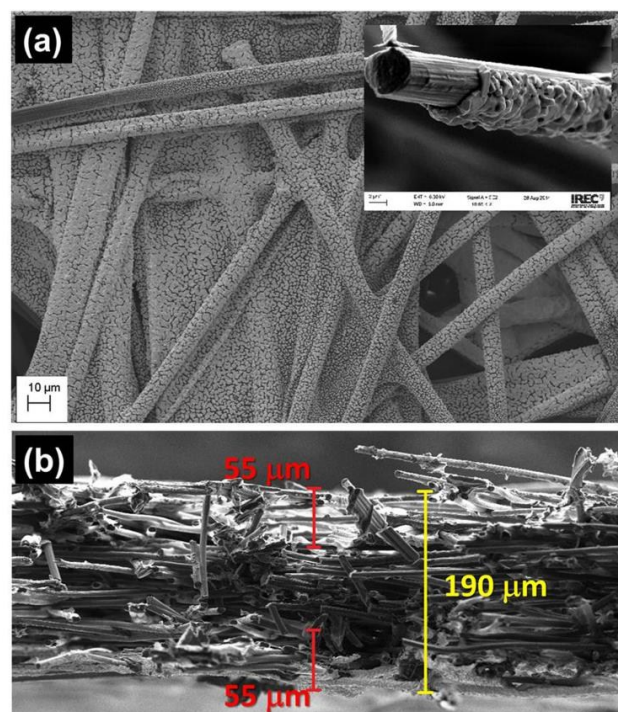


Figure 3. (a) FE-SEM top view image of Sn-GDE electrode obtained by electrodeposition of Sn at 15 mA cm^{-2} for 4.5 C cm^{-2} on C-Toray paper from pyrophosphate solution. Insert shows the Sn deposit on a carbon fiber. (b) FE-SEM cross section of Sn-GDE.

under N_2 gas stream and also when electrode is dipped inside a solution. In the range from 10 to 30 mA cm^{-2} , 15 mA cm^{-2} was estimated to be the optimal current density for a uniform and compact distribution of tin over the carbon fibers (Figure 3a). Chronopotentiometric curve (insert in Figure 1) acquired during electrodeposition at 15 mA cm^{-2} shows a sharp decrease of electrode potential due to charging of the double layer since it is reached the potential where the tin reduction takes place.

Under these conditions, a thickness around $1\text{ }\mu\text{m}$ around a single carbon fiber was confirmed by FE-SEM image. When the

deposition is carried out at 15 mA cm^{-2} , the average Sn loading on GDE measured by weight difference is 2.6 mg cm^{-2} for 4.5 C cm^{-2} , and consequently, the average faradaic efficiency of Sn electrodeposition was 94%. Figure 3b shows the cross-section of the sample, confirming Sn film formation at $50 \pm 5 \mu\text{m}$ inside the porous electrode at both sides of the carbon paper.

X-ray diffraction (XRD) pattern (Figure S2) shows that among its allotropes the catalyst obtained by electrodeposition crystallises in its beta phase with tetragonal structure. Besides the graphite reflection from the C-Toray® paper substrate, the (200) and (101) peaks of β -Sn were the strongest signals observed for the polycrystalline film and all the other peaks well corresponds to the reference pattern.

3.2. Gas diffusion electrode test

Figure 4 presents the comparison of polarization curves of the electroreduction on Glassy Carbon (GC) electrode, pristine gas diffusion electrode (GDE), and electrodeposited Sn on GDE (Sn-GDE) in 0.5 M NaHCO_3 electrolyte buffer under Ar or CO_2 bubbling. The lower current density achieved with GC compared to that obtained with GDE verifies the large active surface area of porous electrode vs. a planar support. Besides, the nearly two times higher current density of Sn-GDE under CO_2 than under Ar (grey and red line, respectively) is attributable to the electroreduction of CO_2 . The standard potential of CO_2 reduction to formate and carbon monoxide are -0.225 and $-0.103 \text{ V}_{\text{RHE}}$ ³⁰ according to reactions in equation (2) and (3), respectively. Hence the overpotential of CO_2 reduction is only 400 and 490 mV for CO and HCOO^- . Furthermore, in comparison to the Ar-saturated solution, the current density increases by 3 times in the presence of CO_2 gas at an overpotential of only 0.8 V. Compared with recent results with a 5 nm size catalyst,²⁴ our electrodeposited Sn catalyst on carbon fibers perform with 0.25 V regardless of the up-scaling challenges at larger electrode dimension (Fig. S3).

Before moving to the targeted electrolysis experiments, we conducted further analyses on the inertness of carbon fibers and final product contribution of the carbonate buffer. Firstly, previous studies showed³¹ that carbon surface alone (glassy carbon, activated carbon and etc.) can reduce CO_2 at sufficiently high potentials. Therefore chronoamperometry tests were conducted with similar flow cell CO_2 R conditions during 10 hours onto pristine GDE under $10 \text{ ml min}^{-1} \text{ CO}_2$ gas flow at $-0.85 \text{ V}_{\text{RHE}}$ in order to validate the inertness of GDE towards CO_2 electroreduction. Secondly, Sn-GDE were tested under the same conditions although Ar gas flow was changed to 10 ml.min^{-1} to confirm that CO_2 in gas form was the true reactant involved in the electroreduction process at the TPI (gas-liquid-solid; triple phase interface) sites but not only between liquid-electrode sites. At the end of 10 hours experiments, 2 and $3 \mu\text{mol h}^{-1}$ of formate (HCOO^-) were detected for GDE and Sn-GDE electrodes, respectively. Those values are equivalent to 24.8 and 36.6 ppm which is within the error limit of HPLC protocols towards formate detection ($< 50 \text{ ppm}$). Therefore, the blank test results can be considered as

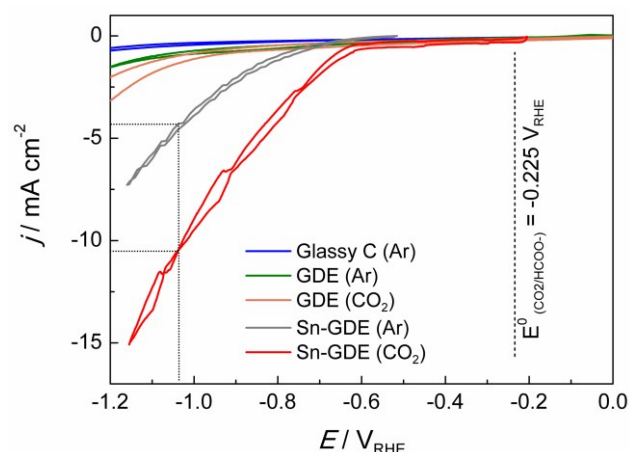


Figure 4. Cyclic voltammogram on glassy carbon (GC), GDE and Sn-GDE under 10 mL min^{-1} Ar or CO_2 gas flow at scan rate 20 mV s^{-1} in 0.5 M NaHCO_3 electrolyte (GC electrode was tested in 3-electrode EC cell with CO_2 bubbling while the other electrodes in filter-press EC cell)

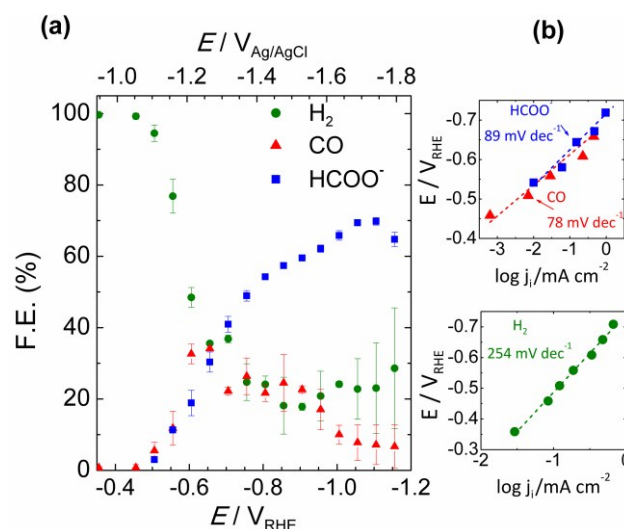


Figure 5. (a) Total faradaic efficiency of CO_2 reduction products at the end of 200 C of charge passed from the external circuit and (b) corresponding Tafel plots for production of HCOO^- , CO and H_2

null in terms of formate faradaic efficiency ensuring that gaseous CO_2 is the active specie.

3.3. CO_2 reduction products and Tafel plot analysis

Total faradaic efficiencies towards formation of HCOO^- and CO/H_2 as liquid and gaseous products, respectively, are given in Figure 5 a. The working electrode potential versus CO_2 conversion to formate frequently produces an “elbow” shape³² which is also observed in our results. As previously discussed by several authors^{16, 18-20, 24, 30, 33, 34}, this is ascribed to a critical limiting step related to competitive hydrogen and carbon monoxide production. So, there is a (1:1:1) product ratio voltage zone around $-0.65 \text{ V}_{\text{RHE}}$ where Sn-GDE can convert CO_2 into up to $32 \pm 2.7 \%$ CO detected by an online GC set-up, $30 \pm 2.8 \%$ HCOO^- and the rest into H_2 . Increasing this voltage, the product ratio changes, being the production of HCOO^- favoured in the -0.65 - $-1.1 \text{ V}_{\text{RHE}}$ range. Beyond that potential, selectivity shifts again towards H_2 production. So, by modulating the working

conditions, a faradaic efficiency for HCOO^- , detected by HPLC, as high as $71 \pm 1.1\%$ could be obtained, reaching $82 \pm 2.0\%$ of total CO_2 reduced to C-products, including CO ($6 \pm 4.5\%$). Figure S4 highlights the ratio control on the CO to H_2 (syngas) with a reliable stability for 2 hours for the voltages between -0.65 to $-0.105 \text{ V}_{\text{RHE}}$.

Tafel slopes of the CO_2 reduction process are calculated from analogous data obtained applying chronoamperometry tests of 200 Coulomb in 50 mL catholyte. Plotting the logarithm of partial current of each product against the electrode potential gives its Tafel slope value. Figure 5b shows the reduction of CO_2 to HCOO^- and CO giving, respectively, a slope of 89 and 78 mV dec^{-1} at the low potential range. As expected, Tafel slope value of H_2 was found to be much higher, 254 mV dec^{-1} , which is due to the low adsorption capability resulting in higher overpotential and sluggish kinetics towards H_2 evolution on Sn metal. Those findings are in good correlation with the Tafel values of Kanan et. al.¹⁷ which is 74 and 77 mV dec^{-1} for HCOO^- and CO, respectively. Our initial findings, with comparable Tafel slope and on-set voltage values^{17, 35, 36}, are the indicator of a competing rate determining step prior to electron transfer to CO_2 forming $\text{CO}_2^{\bullet-}$ radical.

3.4. Faradaic efficiency and hydrodynamic conditions

After verifying the catalytic performance of electrodeposited Sn on carbon fiber-based gas diffusion electrode, next step is to take advantage of the possibility of tuning the flow system, i.e. ratio of gas and liquid flows, and observe how mass transport can affect CO_2 reduction. The influence of hydrodynamic conditions on mechanisms involved in the reaction intermediates has been well studied.³⁷ These conditions may occur either because the electrode itself is in motion respect to the solution, i.e. rotating disk electrode, or because there is a forced solution flow passing through a stationary electrode, i.e. channel electrodes or bubbling electrodes.³⁸ The advantage is that a steady state is attained very quickly, meaning a diffusion layer would be formed at a certain distance from the electrode (diffusion layer, δ) by forced convection. In that state, the current can be related to flow rates, by means of flux of CO_2 gas and the electrolyte that acts as proton source. Therefore, changes in formate production rate could take place by changing hydrodynamic conditions (gas and liquid flow rates) and electronic energies (applied potential or current) if some of these parameters are limiting these processes.

Initially, a cyclic voltammetry test was conducted at different CO_2 to Ar proportions, and CO_2 gas amount was increased from 0 to 100 %. A clear distinction can be seen in the current density vs potential plots in Figure S5. The increment of CO_2 gas flow from 10 to 100 % resulted in one fold higher current density (0.69 to 8.3 mA cm^{-2}) when the current generated under Ar was subtracted from CO_2 to obtain partial current due to CO_2 electroreduction, as shown in Figure 6. Furthermore, when gas and liquid flow rates are equal ($\text{G/L} = 1$), net current density reaches 8.13 mA cm^{-2} for pure CO_2 inlet at $-1.1 \text{ V}_{\text{RHE}}$. The further increase of gas flow rate above the

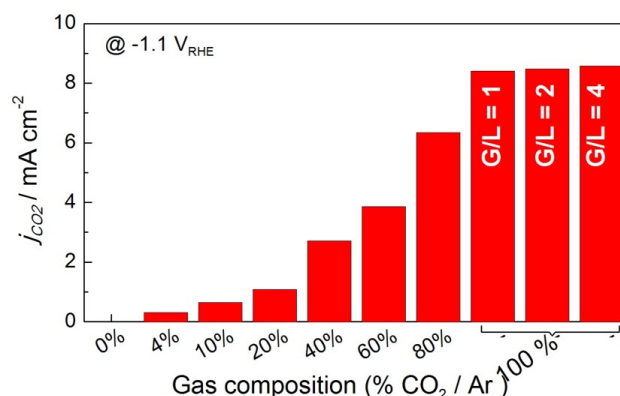


Figure 6. Histogram of net current density for CO_2 reduction on Sn-GDE obtained by subtracting the current density value of Ar from CO_2 at $-1.1 \text{ V}_{\text{RHE}}$ in the CV scans (figure S5). Data recorded in the filter-press cell in 0.5 M NaHCO_3 (50 mL min^{-1}) increasing the amount of gas by CO_2 percentage in Ar gas flow (total flow 50 mL min^{-1}). For G/L 2 and 4, 100 and 200 mL min^{-1} of gas flow was used.

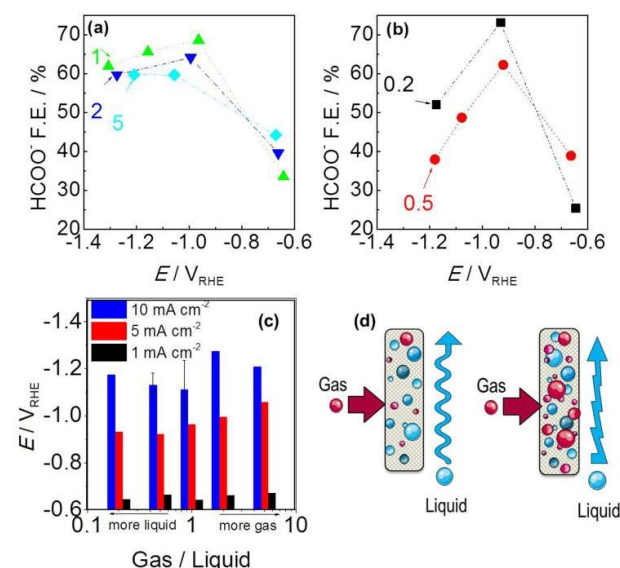


Figure 7. Faradaic efficiency of formate versus Sn-GDE electrode potential: (a) Gas/Liquid = 1, 2 or 5 and (b) Gas/Liquid = 0.2 or 0.5 in 0.5 M NaHCO_3 for 200 C electrolysis (c) CO_2 gas to 0.5 M NaHCO_3 electrolyte flow ratio effect on Sn-GDE electrode potential (d) Schematic of gas and liquid flow over Sn-GDE, at $\text{G/L} = 0.2$ and 0.5 and $\text{G/L} = 1, 2$ and 5 , left and right parts respectively.

liquid flow rate shows a smaller increase in the current density, 8.47 and 8.58 mA cm^{-2} – for $\text{G/L} = 2$ and 4 as 100 and 200 mL min^{-1} as CO_2 gas flow respectively while liquid flow is 50 mL min^{-1} . This result proves that not only the increase of the CO_2 gas but also G/L flow ratio is essential to promote higher current densities. Here, the conversion of CO_2 into formate (HCOO^-) must be in relation to the liquid flow because the electrolyte is the critical component for the protonation of the intermediate specie shown in equation (3).

For a further understanding, electrolysis tests for 200C were conducted at different cell currents (1 , 5 and 10 mA cm^{-2}) and gas-to-liquid (G/L) flow rates while individual electrode potential values were recorded during electrolysis. For the selected current densities, we have explored 5 different G/L

ratios by modifying volumetric flow of CO_2 gas and electrolyte from 5 to 50 mL min^{-1} resulting in: 0.5, 1, 2 and 5 in terms of gas-to-liquid (G/L) flow ratios

A thorough product analysis by liquid chromatography revealed a dependence of gas to liquid ratio versus electrode potential which is shown in Figure 7 (a) and (b). All the lines show an arc-shaped dependence of formate efficiency to electrode potential. The most significant effect can be seen for the red and black curve, 0.2 and 0.5 G/L ratio, that the amount of CO_2 gas is not sufficient for reaching the overpotential required to convert CO_2 into HCOO^- . While ratio of 1 provides higher current efficiency, still the reaction is under a rate control mechanism. The further increase of the gas to liquid ratio gives a lower faradaic efficiency for formate in a related trend: $1 > 2 > 5$. Here a remark should be given for the rising electrode potentials with the increment of G/L value, in Figure 7c. It is well-known that, higher turbulence at the electrode-electrolyte interface hinders the complete utilization of the electrode surface. High amount bubbles most probably accumulate and locally block the active sites of the tin catalyst (Fig. 7d). Moreover, a contribution to the electrolyte resistance was revealed at the electrode interface which is shown by the increase of the electrode potential in Fig 7 (c).³⁹

Moreover an improvement in faradaic efficiency was observed for 0.2 compared to 0.5. It seems that at low G/L flow ratio, where the liquid flow is superior to gas flow, there is sufficient time for the adsorption and stabilization of $\text{CO}_{2(g)}$ at the electrode surface before the consecutive step of electron uptake. Also, several (experimental and computational) studies highlighted that proton uptake of the CO_2^- radical could be a rate determining step and the faradaic efficiency for producing formate is promoted by proton existence at the surface layer and hydrogenating the carbon atom.^{20, 33, 35}

3.5. Stability and cost of formate production

The catalytic activity of the Sn deposit was tested for 6 hours, results are shown in Figure S6 (a) where the dotted line corresponds to 100 % faradaic efficiency of formate conversion from CO_2 . A stable formate production yield was attained (at 1 to 10 mA cm^{-2} applied current densities) during the whole experiment. Moreover, experiments at 1 and 5 mA cm^{-2} were held to longer times in order to maintain the analytical protocol by preventing a high product saturation altering the acidity of the electrolyte. The longstanding activity is attributed to the chosen deposition batch providing a catalyst coating free of impurities (proven by the EDX scan in Fig S6) and a well crystallized, compact catalyst film. Likewise, we haven't observed any significant catalyst losses in weight. Previous works (Li & Oloman -S1-) used Sn deposited on Cu mesh electrodes having 50 – 86 % HCOOH conversion at a high expense of -4 to -5.8 V cell voltages but they report low catalytic stability in their work (catalyst deteriorating after about 20 min operation) was related to the loss of Sn from the mesh surface.⁴⁰ In our case, it seems that there is not any

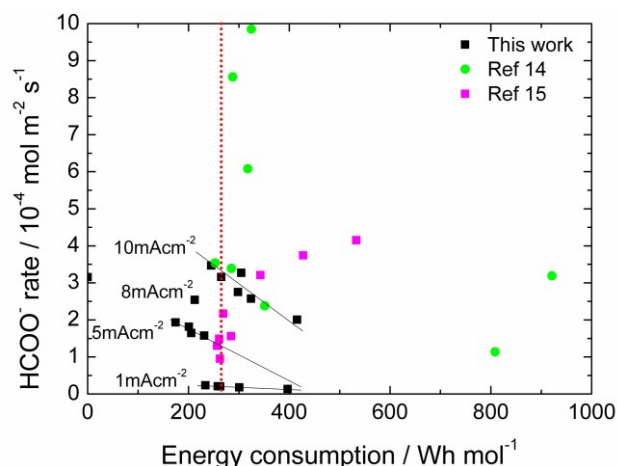


Figure 8. Energy consumption of CO_2 R to formate using Sn-GDE in filter-press EC cell at different production rates. Data from this work and references 14-15.

internal stress at the grain boundaries of Sn deposit since any long crack formation have been observed.

A final figure of merit to be highlighted is the energy efficiency of the process. Taking into account the combustion energy associated to formic acid (70.7 Wh mol^{-1}), a threshold of 250 Wh mol^{-1} can be set, since the energy efficiency of the process would be 35%. In Figure 8 it is shown the results of this work compared with previous literature that use a similar cell configuration but with a Sn-GDE obtained by spraying an ink (Sn nanoparticles + Nafion® solution) on C-Toray.^{14, 15} As it can be seen, for the same applied current density, there is a wide range of values. Here, besides the current density, the faradaic efficiency of the process has a direct impact on the energy efficiency of the process, higher F.E. implies a higher HCOO^- rate and, consequently, lower energy consumption. Besides this, our binder free Sn-GDE electrode shows a lower resistance (1.2Ω , see S3) resulting in a lower iR drop whereas reported values range 5-7 Ω using ink based electrodes (Wu, Jingjie, S1).¹⁶ In our process, there is an optimum point in the range from 2 to 4 $10^{-4} \text{ mol m}^{-2} \text{ s}^{-1}$ where the required energy can be lower than 200 Wh per mol (whereas results from bibliography show higher production yield up to 1 $\text{mmol m}^{-2} \text{ s}^{-1}$ but associated to an energy consumption higher than 250 Wh mol^{-1} that limits its practical application.

4. Conclusions

The electrodeposition of tin catalyst on carbon fibers, free of additives and up-scalable for gas diffusion electrodes, has been proved as a successful alternative methodology for preparing gas diffusion electrodes feasible for CO_2 electroreduction to formate. The highest faradaic efficiency for HCOO^- detected by HPLC was $71 \pm 1.1 \%$, being fully stable at least for 6 hours, reaching to $82 \pm 2.0 \%$ of total CO_2 conversion to C-products (HCOO^- and CO). In the electrochemical flow cell, faradaic efficiencies were also dependent on the gas to liquid flow ratio, due to the turbulence promoted at the electrode by the CO_2 flow. At low gas to liquid flow ratio; greater the electrolyte

flow provided higher faradaic efficiency ($0.2 > 0.5$) which could be due to the residence time of the $\text{CO}_2^{\bullet-}$ intermediate specie. As this process is likewise high energy consuming, it is relevant to equilibrate its production yield with the energy consumption. According to the reported data, by taken care of the electrocatalyst synthesis procedure on gas diffusion electrode it is validated that it is possible to decrease energy consumption below 200 Wh mol^{-1} , maintaining relative high production yields by surface and time units, which converts the electroreduction method into a significant and competitive alternatives for formate production from CO_2 electroreduction.

Acknowledgements

This work was supported by Repsol, S.A. Authors from IREC and UB belong to the M-2E (Electronic Materials for Energy, 2014SGR1638) Consolidated Research Group and the XaRMAE network of excellence on Materials for Energy of the "Generalitat de Catalunya". IREC also acknowledges additional support by the European Regional Development Funds (ERDF, FEDER) and by MINECO projects ENE2012-3651 and MAT2014-59961. EI thanks to AGAUR for his PhD grant (FI-2013-B-00769).

Notes and references

- G. Centi, E. A. Quadrelli and S. Perathoner, *Energy Environ. Sci.*, 2013, **6**, 1711-1731.
- A. J. Bard, R. Parsons and J. Jordan, *Standard potentials in aqueous solution*, CRC press, 1985.
- J. Medina-Ramos, R. C. Pupillo, T. P. Keane, J. L. DiMeglio and J. Rosenthal, *J. Am. Chem. Soc.*, 2015, **137**, 5021-5027.
- Q. Wang, H. Dong and H. Yu, *RSC Adv.*, 2014, **4**, 59970-59976.
- C. W. Li, J. Ciston and M. W. Kanan, *Nature*, 2014, **508**, 504-507.
- K. P. Kuhl, T. Hatsukade, E. R. Cave, D. N. Abram, J. Kibsgaard and T. F. Jaramillo, *J. Am. Chem. Soc.*, 2014, DOI: 10.1021/ja505791r.
- B. Innocent, D. Pasquier, F. Ropital, F. Hahn, J. M. Léger and K. B. Kokoh, *Appl. Catal. B*, 2010, **94**, 219-224.
- Z. M. Detweiler, J. L. White, S. L. Bernasek and A. B. Bocarsly, *Langmuir*, 2014, **30**, 7593-7600.
- Y. Hori, H. Wakebe, T. Tsukamoto and O. Koga, *Electrochim. Acta*, 1994, **39**, 1833-1839.
- B. C. H. Steele and A. Heinzl, *Nature*, 2001, **414**, 345-352.
- A. P. G. Kieboom, *Recl. Trav. Chim. Pays-Bas*, 1988, **107**, 685-685.
- G. K. S. Prakash, F. A. Viva and G. A. Olah, *J. Power Sources*, 2013, **223**, 68-73.
- M. N. Mahmood, D. Masheder and C. J. Harty, *J. Appl. Electrochem.*, 1987, **17**, 1159-1170.
- A. Del Castillo, M. Alvarez-Guerra, J. Solla-Gullón, A. Sáez, V. Montiel and A. Irabien, *Appl. Energy*, 2015, **157**, 165-173.
- A. Del Castillo, M. Alvarez-Guerra and A. Irabien, *AIChE J.*, 2014, **60**, 3557-3564.
- J. Wu, P. P. Sharma, B. H. Harris and X.-D. Zhou, *J. Power Sources*, 2014, **258**, 189-194.
- Y. Chen and M. W. Kanan, *J. Am. Chem. Soc.*, 2012, **134**, 1986-1989.
- J. Wu, F. G. Risalvato, M. Shuguo and X.-D. Zhou, *J. Mater. Chem. A*, 2014, **2**, 1647-1651.
- J. Wu, F. G. Risalvato, P. P. Sharma, P. J. Pellechia, F.-S. Ke and X.-D. Zhou, *J. Electrochem. Soc.*, 2013, **160**, F953-F957.
- J. Wu, F. G. Risalvato, F.-S. Ke, P. J. Pellechia and X.-D. Zhou, *J. Electrochem. Soc.*, 2012, **159**, F353-F359.
- S. Lee, J. D. Ocon, Y. I. Son and J. Lee, *J. Phys. Chem. C*, 2015, **119**, 4884-4890.
- Y. Fu, Y. Liu, Y. Li, J. Qiao and X. D. Zhou, *ECS Trans.*, 2015, **66**, 53-59.
- C. Zhao, J. Wang and J. B. Goodenough, *Electrochem. Commun.*, 2016, **65**, 9-13.
- S. Zhang, P. Kang and T. J. Meyer, *J. Am. Chem. Soc.*, 2014, **136**, 1734-1737.
- Y. Hori, H. Konishi, T. Futamura, A. Murata, O. Koga, H. Sakurai and K. Oguma, *Electrochim. Acta*, 2005, **50**, 5354-5369.
- M. Alvarez-Guerra, A. Del Castillo and A. Irabien, *Chem. Eng. Res. Des.*, 2014, **4**, 692-701.
- M. Alvarez-Guerra, S. Quintanilla and A. Irabien, *Chem. Eng. J.*, 2012, **207-208**, 278-284.
- Q. Wang, H. Dong and H. Yu, *J. Power Sources*, 2014, **271**, 278-284.
- M. Shafiei and A. T. Alpas, *J. Power Sources*, 2011, **196**, 7771-7778.
- B. P. Sullivan, K. Krist and H. Guard, *Electrochemical and electrocatalytic reactions of carbon dioxide*, Elsevier, 1992.
- R. M. Hernández, J. Márquez, O. P. Márquez, M. Choy, C. Ovalles, J. J. Garcia and B. Scharifker, *J. Electrochem. Soc.*, 1999, **146**, 4131-4136.
- M. Jitaru, D. Lowy, M. Toma, B. Toma and L. Oniciu, *J. Appl. Electrochem.*, 1997, **27**, 875-889.
- W. Lv, R. Zhang, P. Gao and L. Lei, *J. Power Sources*, 2014, **253**, 276-281.
- R. P. S. Chaplin and A. A. Wragg, *J. Appl. Electrochem.*, 2003, **33**, 1107-1123.
- C. Cui, J. Han, X. Zhu, X. Liu, H. Wang, D. Mei and Q. Ge, *J. Catal.*, 2016, DOI: 10.1016/j.jcat.2015.12.001.
- C. Cui, H. Wang, X. Zhu, J. Han and Q. Ge, *Sci. China Chem.*, 2015, **58**, 607-613.
- J. Newman and K. E. Thomas-Alyea, *Electrochemical systems*, John Wiley & Sons, 2012.
- A. J. Bard and L. R. Faulkner, *Electrochemical methods: fundamentals and applications*, Wiley New York, 1980.
- H.-R. M. Jhong, S. Ma and P. J. A. Kenis, *Curr. Opin. Chem. Eng.*, 2013, **2**, 191-199.
- H. Li and C. Oloman, *J. Appl. Electrochem.*, 2005, **35**, 955-965.

The binder free Sn-GDE obtained by electrodeposition allows CO_2 electroreduction to formate with low energy consumption for sustainable fuel production.

